Polyelectrolytes Multilayers to Modulate Cell Adhesion: A Study of the Influence of Film Composition and Polyelectrolyte Interdigitation on the Adhesion of the A549 Cell Line

Nicolás E. Muzzio, Miguel A. Pasquale, Danijela Gregurec, Eleftheria Diamanti, Marija Kosutic, Omar Azzaroni, Sergio E. Moya*

Polyelectrolyte multilayers (PEMs) with different polycation/polyanion pairs are fabricated by the layer-by-layer technique employing synthetic, natural, and both types of polyelectrolytes. The impact of the chemical composition of PEMs on cell adhesion is assessed by studying cell shape, spreading area, focal contacts, and cell proliferation for the A549 cell line. Cells exhibit good adhesion on PEMs containing natural polycations and poly(sodium 4-styrenesulfonate) (PSS) as polyanion, but limited adhesion is observed on PEMs fabricated from both natural polyelectrolytes. PEMs are then assembled, depositing a block of natural polyelectrolytes on top of a stiffer block with PSS as polyanion. Cell adhesion is enhanced on top of the diblock PEMs compared to purely natural PEMs. This fact could be explained by the interdigitation between polyelectrolytes from the two blocks. Diblock PEM assembly provides a simple means to tune cell adhesion on biocompatible PEMs.

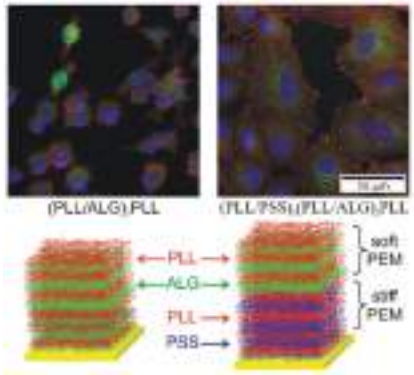

1. Introduction

Featured materials employing natural and synthetic polymers are increasingly being used for the modulation of cell functions based on diverse strategies that modify the physical and chemical properties of the substrate interacting with the cells, such as the substrate composition, surface energy, wettability, charge, roughness, stiffness, and deformability, as well as the presence of patterns.[1] For this scope, a large amount of different materials mimicking aspects of the interactions between cells and their environment has been employed: natural and synthetic polyelectrolyte multilayers (PEMs), protein-coated polymeric substrates with tunable stiffness,[2] biocompatible hydrogels that can be biochemically and mechanically altered by chemical functionalization or by changing hydrogel cross-linking density, respectively.[3] Furthermore, microgels have been used alone to fabricate thin film substrates or as constitutive units combined with polyelectrolytes.[4] On the other hand, microenvironmental cues that affect cell functions and appear in 3D cell culture can be reproduced employing micropatterned substrate containing regions with cell-adhesive material of well-defined shape

N. E. Muzzio, Dr. M. A. Pasquale, Dr. O. Azzaroni
Instituto de Investigaciones Fisicoquímicas Teóricas y Aplicadas (INIFTA), (UNLP, CONICET)
Sucursal 4, Casilla de Correo 16
1900 La Plata, Argentina
D. Gregurec, E. Diamanti, Dr. M. Kosutic, Dr. S. E. Moya
Soft Matter Nanotechnology Group
CIC biomaGUNE, Paseo Marimón 182 C
20009 San Sebastián Gipuzkoa, Spain
E-mail: smoya@cicbiomagune.es

DOI: 10.1002/mabi.201500275

and spatial distribution, and by including nanofeatures that alter the mechanical properties of the environment.[5]

The layer-by-layer (LbL) technique offers a simple and effective means for the engineering of surfaces based mainly on the electrostatically driven assembly of polyelectrolytes.[6,7] In the LbL technique polyelectrolytes of opposite charge are sequentially assembled on top of a planar or colloidal charged surface.[8] In addition to polyelectrolytes, other molecules,[9,10] nanoparticles,[11] lipid vesicles,[12] and even cells[13] can be assembled on top of the multilayers or by replacing selected layers provided these are charged or may interact with previous and subsequent assembled layers by any other type of interaction, i.e., coordination chemistry or hydrogen bonding. The LbL assembly results in the fabrication of thin films with nanoscale controlled composition in the vertical direction.

Polyelectrolytes of natural origin, such as poly-L-lysine (PLL), hyaluronic acid (HA), alginate, etc., are very appealing for the modification of surfaces for biological applications, among them, for cell tissue engineering.[14,15] When assembled in PEMs, these polyelectrolytes form a biocompatible cushion on which growth factors, proteins, peptide sequences, and other biomolecules can be covalently bonded or assembled, controlling cell functionalities such as cell growth, adhesion, and migration.[16] Altogether LbL technique represents a powerful strategy for modifying surfaces and endowing them with specific components. PEMs are very promising materials to be used in the formulation of drug delivery systems,[17,18] single cell analysis for diagnostics, and fundamental cell biology studies as their chemical and physical properties can be modified conveniently.[19]

Cell adhesion plays indeed a key role in many physiological and pathological processes such as wound healing[20] and bacterial infections,[21] as well as in the progression of tumors.[22] Gaining control on the adhesion properties of a surface is fundamental for tissue engineering and medical implants, and for the development of strategies for drug delivery.[23] Cell adhesion is possible if the substrate stiffness is enough to generate forces to balance intracellular tension forces generated by stress fibers.[24] Furthermore, matrix stiffness regulates cancer cell malignancy through a complex mechanism.[25]

Selective adhesion between endothelial and muscle cells has been achieved by changing the mechanical properties of substrates by coating with different PEMs.[26] In this case, stiffness modulation was based on the fact that cells can sense the stiffness of objects that are not in direct contact,[27] depending on the number of polyelectrolyte layers assembled as well as on their chemical and physical properties.

Other strategies can be applied for the enhancement of cell adhesion on PEMs based on the increase in the substrate stiffness via changes in the chemical composition of the film. The crosslinking between polyelectrolytes[15,41] or the addition of nanoparticles[11,15] has been successfully applied in this regard. Furthermore, cell adhesion can be improved on substrates assembled with the combination of different blocks of PEMs. In this case, HT29 cell adhesion gradually increased when soft natural PEMs made of PLL and HA were successively capped with poly(sodium 4-styrenesulfonate) (PSS) and blocks made of one and two bilayers of PSS and poly(allylamine hydrochloride) (PAH).[28] This fact was attributed to the increase in the elastic modulus and the viscosity of the capped films, as it has been demonstrated by indentation measurements.[29] It was suggested that the increase in stiffness was due to the penetration of PSS into the underlying film made of PLL and HA, which was inferred from infrared spectroscopy. A similar approach has been employed to investigate the relationship between elasticity and replication and transcription in PtK2 cells.[30] In this paper, the apparent elastic modulus of PEMs was varied from 0 to 500 kPa by assembling an increasing number of bilayers assembled with PAH and PSS on top of a block of 24 PLL and HA based bilayers, and the trigger of distinct cell functions was mechanistically described in relation to the resulting substrate stiffness. In another paper, a cooperative effect has been reported when chitosan (CHI) and HA PEMs were combined with a certain amount of CHI and polyacrylic acid (PAA) PEMs, obtaining a considerable increase in the Young modulus.[31] The authors postulated the formation of a new interaction between polyelectrolytes due to the interdigitation process.

Although several articles have addressed the use of multilayers for many medical applications,[15,32] no systematic study about the impact of the chemistry of PEMs on cell adhesion has been reported. The chemical composition of PEMs is directly related to their mechanical properties, which are fundamental to controlling adhesion. PEMs properties are also a combination of the properties of the polycations and polyanions forming the multilayers. PEMs with the same top layer but different underlying counter polyelectrolytes may have different properties and, consequently, they may interact differently with cells. Also, a different composition of the PEMs along the vertical direction, i.e., different polyelectrolyte composition at the bottom and the top of the PEMs, can influence the interaction with cells as well. It is indeed interesting to know how far the properties of inner layers are sensed by cells interacting with the PEMs as PEMs could be produced using, for example, stiffer polyelectrolytes of synthetic origin and softer biopolymers on the top layers, in contrast with the sequence used in refs. [28–31]. In this way, the top layers facing the cells would be biocompatible. Also, the film properties could be tuned for biocompatibility and stiffness, which is fundamental for the applications of PEMs related to cell adhesion control. We

have addressed these issues in this paper by varying the chemical composition of PEMs, combining synthetic and natural polyelectrolytes, by changing the composition of PEMs at defined positions, and fabricating PEMs with two different blocks assembled from diverse polycations and polyanions with different number of layers.

2. Experimental Section

2.1. Materials and Reagents

PLL solution (M_w 70–150 kDa, P4707), PSS (average M_w ≈70 kDa, 243051), PAH (average M_w ≈58 kDa, 283223), branched polyethylenimine (PEI; average M_w ≈25 kDa by LS, average M_w ≈10 kDa by GPC, 408727), poly(diallyldimethylammonium chloride) solution (PDADMAC; average M_w ≈200–350 kDa, 409022), poly(acrylic acid) solution (PAA; average M_w ≈100 kDa, 523925), dextran sulfate sodium salt from Leuconostoc spp. (DEX; average M_w 9–20 kDa, D6924), sodium chloride, HEPES sodium salt, phosphate buffered saline (PBS; D1408), bovine serum albumin (BSA), anti-mouse IgG-FITC antibody (F0257), sodium dodecyl sulfate (SDS; L6026), Triton X-100 (T8787), Tween-20 (P9416), thiazolyl blue tetrazolium bromide (MTT; M5655), and dimethyl sulfoxide (DMSO; 472301) were purchased from Sigma-Aldrich. Sodium Alginate (ALG; Cat. No. 17777-0050), CHI (M_w 100–300 kDa, Cat. No. 349051000), and HA (M_w 1500–2200 kDa, Cat. No. 251770010) were acquired from Acros Organics.

Actin Cytoskeleton and Focal Adhesion Staining Kit (FAK100) and anti-fade mounting solution were obtained from Millipore. RPMI 1640 with L-glutamine was from Lonza and fetal bovine serum (FBS) was purchased from Fisher. Nanopure water was obtained using the Barnstead Nanopure Ultrapure Water Purification System.

2.2. Multilayer Films Preparation via LbL Assembly

All polyelectrolyte solutions were prepared at a concentration of 1 mg mL^{-1} in a 150×10^{-3} M NaCl, 10×10^{-3} M HEPES pH = 7.4 buffer (with the exception of CHI which was prepared in a 150×10^{-3} M NaCl, 10×10^{-3} M acetic acid buffer, and adjusted to pH 5.0) and filtered through a 0.45 μm filter. These assembling conditions were selected because it is likely to assure PEMs stability in physiological conditions.

Before use the cover glasses were cleaned as reported previously.[33] Briefly, the glasses were immersed in 10×10^{-3} M SDS for 3 h, rinsed in sterile water three times, treated with 0.1 M HCl overnight, and thoroughly rinsed in water. All PEMs were assembled with 15 layers of polyelectrolytes, being the first and the last layer always a polycation. Polycations and polyanions were alternately assembled by manual dipping at 24 °C and were allowed to assemble for 15 min. After each layer deposition, films were rinsed three times in water.

2.3. Atomic Force Microscopy

PEMs were prepared for atomic force microscopy imaging as described in the previous section. After the LbL assembly, samples were rinsed with nanopure water and left to dry in air. The morphology of PEMs was obtained using an AFM from Nanowizard II AFM (JPK, Berlin, Germany). Images were collected in tapping mode with TESP-V2 cantilever (Bruker, AFM Probes) with nominal spring constant of 40 N m^{-1} and oscillated near a resonant frequency in the range of 280 to 320 kHz.

2.4. Quartz Crystal Microbalance with Dissipation Measurements

The deposition of the polyelectrolytes was monitored via the quartz crystal microbalance with dissipation (QCM-D) Q-Sense E4 system. The coating of the PEM film was conducted on SiO_2 (50 nm) coated quartz crystals (5 MHz, Q-Sense). Polyelectrolyte solutions were injected in the 4-sensor chamber with the help of a peristaltic pump and left under incubation for 10 min. After stabilization of the frequency another 10 min rinsing with 150×10^{-3} M NaCl, 10×10^{-3} M Hepes buffer (pH = 7.4) was performed. Experiments were conducted at 23 °C.

2.5. Cell Culture

A549 epithelial cells, a human lung carcinoma cell line, were grown in RPMI medium supplemented with 10% FBS (and antibiotics) and incubated at 37 °C in a 5% CO_2 humidified atmosphere. This cell line was used in various basic studies of polyelectrolyte coated surfaces.[17,18]

For adhesion assays, glass and films were placed into Petri dishes 35 mm in diameter (Falcon) and UV-sterilized for 1 h,[34] a process widely used and from which no reports indicating significant changes in the PEMs properties are known. Then, 5×10^4 cells in 3 mL culture medium were seeded on top.

2.6. Quantification of Cell Adhesion

To quantify cell adhesion and spreading characteristics, cell contours were manually traced using a Wacom graphic tablet and analyzed using Image Pro Plus 6.0 software, Media Cybernetics Inc. Cell area (in μm^2), aspect ratio (ratio between major axis and minor axis of an ellipse with area equivalent to that of the cell) was determined.[35] An aspect ratio close to 1 corresponds to a rounded cell, whereas higher values are associated with cells having a tapered morphology. Differences in the average cell adhesion area and morphological parameters for each PEM and those obtained on glass were evaluated utilizing one-way analysis of variance (ANOVA) and Fisher test with a significance level $p = 0.05$.

2.7. MTT Cell Proliferation Assay

For MTT experiments, films were assembled in 14 mm circle cover slips and placed in 24-well polystyrene plates. Approximately 2.5×10^4 cells were seeded adding 1 mL of medium. After 24, 48, and 72 h incubation, 80 μL of MTT solution (5 mg mL^{-1} in 10×10^{-3} M PBS) was added into each well. Cells were incubated in the presence of the MTT solution for 3 h at 37 °C. Then, the culture medium was completely removed and the formazan products were solubilized by adding 600 μL of DMSO to each well. The

absorbance spectra were measured at 550 nm by a plate reader (Genios Pro) and the viability was expressed as cell number. Measurements were repeated three times and the mean value and its standard deviation were reported for each condition.

2.8. Cell Immunostaining

Fluorescent staining of vinculin, actin, and cell nucleus was carried out to study cell adhesion. The staining was performed following the protocol described in the Actin Cytoskeleton and Focal Adhesion Staining Kit user manual. Cultured cells were washed with washing buffer, PBS containing 0.05% Tween-20, and fixed with 4% paraformaldehyde. Then, glass cover slips were washed and cells were permeabilized with 0.1% Triton X-100 in PBS for 5 min. After washing, blocking solution, 1% BSA in PBS, was applied for 30 min. Then, the anti-vinculin antibody diluted in blocking solution was added and incubated for 1 h, followed by washing with buffer. The anti-mouse IgG-FITC conjugated antibody (secondary antibody) diluted in PBS was added to the samples and incubated for 1 h. TRITC-conjugated Phalloidin was incubated simultaneously with the secondary antibody for double labeling. After washing, nuclei counterstaining was performed incubating cells with DAPI for 5 min. The samples were washed and mounted on a slide by using anti-fade mounting solution. Stained cells were observed by Confocal Laser Scanning Microscope (Carl-Zeiss LSM 10 META).

3. Results

3.1. (Polycation/Polyanion)$_n$Polycation PEMs

For each selected polycation we fabricated PEMs with the following polyanions: ALG, DEX, HA, PAA, and PSS. As polycations we chose: PLL, CHI, PEI, PAH, and PDADMAC. AFM imaging was used to prove the complete coating of glass with the different PEMs. In Figure 1 we can observe AFM images of PSS/PAH, PLL/ALG, and CHI/HA as example of PEMs made upon synthetic and natural polyelectrolytes. The images in dry state show a complete polymer coating on the glass surface in all cases. For each PEM the topology of the surface is different reflecting the characteristics of the different polyelectrolyte involved and the interactions among them. The assembly of the different PEMs studied was followed by the QCM-D technique, shown in the Supporting Information. Data are presented for each polycation varying the polyanion composition. All curves show a continuous growth for the PEMs, though the type of growth varies for each polycation in relation with the polyanion. For the same polycation depending on the polyanion growth is lineal or supralineal without showing a clear trend among them (Figures S1–S3, Supporting Information).

3.1.1. Cell Morphology and Adhesion

Cell adherence studies were performed on PEMs with a positively charged polyelectrolyte as outermost layer and using glass surfaces as control samples. The cell adhesion area was normalized considering the cell area on glass, $620 \pm 20\ \mu m^2$, as reference.

In Figures 2 and 3 we can observe representative images of A549 cells grown for 48 h on PEMs with PLL (Figure 2) and PAH (Figure 3) as polycations and with all the polyanions studied. PLL and PAH were chosen as examples of natural and synthetic polycations, respectively.

As we can appreciate in Figure 4, the normalized cell adhesion area depends on the PEM composition. By changing the nature of the polyanion for each terminating polycation, PEMs with different cell adhesion properties were obtained. For PEMs assembled with PLL as polycation, the normalized average cell spreading area decreased to about 0.4 with ALG, HA, or DEX as polyanion and to 0.7 with the polyanion PAA. On PEMs assembled with the polycation PAH, the normalized average cell area was lower than on glass for all tested polyanions. In this case, values lower than 0.4 were obtained with HA and PAA, in the range 0.4–0.7 for ALG and DEX, and about 0.8 for PSS as polyanion. On (CHI/HA)$_7$CHI multilayers, the cell spreading area was larger than on glass, but it was smaller on PEMs assembled with CHI as polycation and ALG, DEX, and PAA as polyanion, with values in the

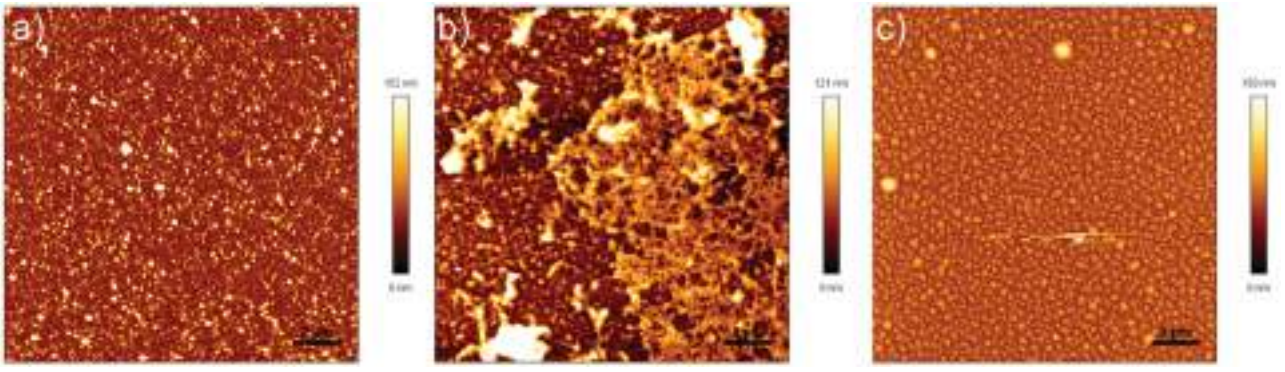

Figure 1. AFM images in dry state of PEMs of a) PSS/PAH, b) PLL/ALG, and 3) CHI/HA.

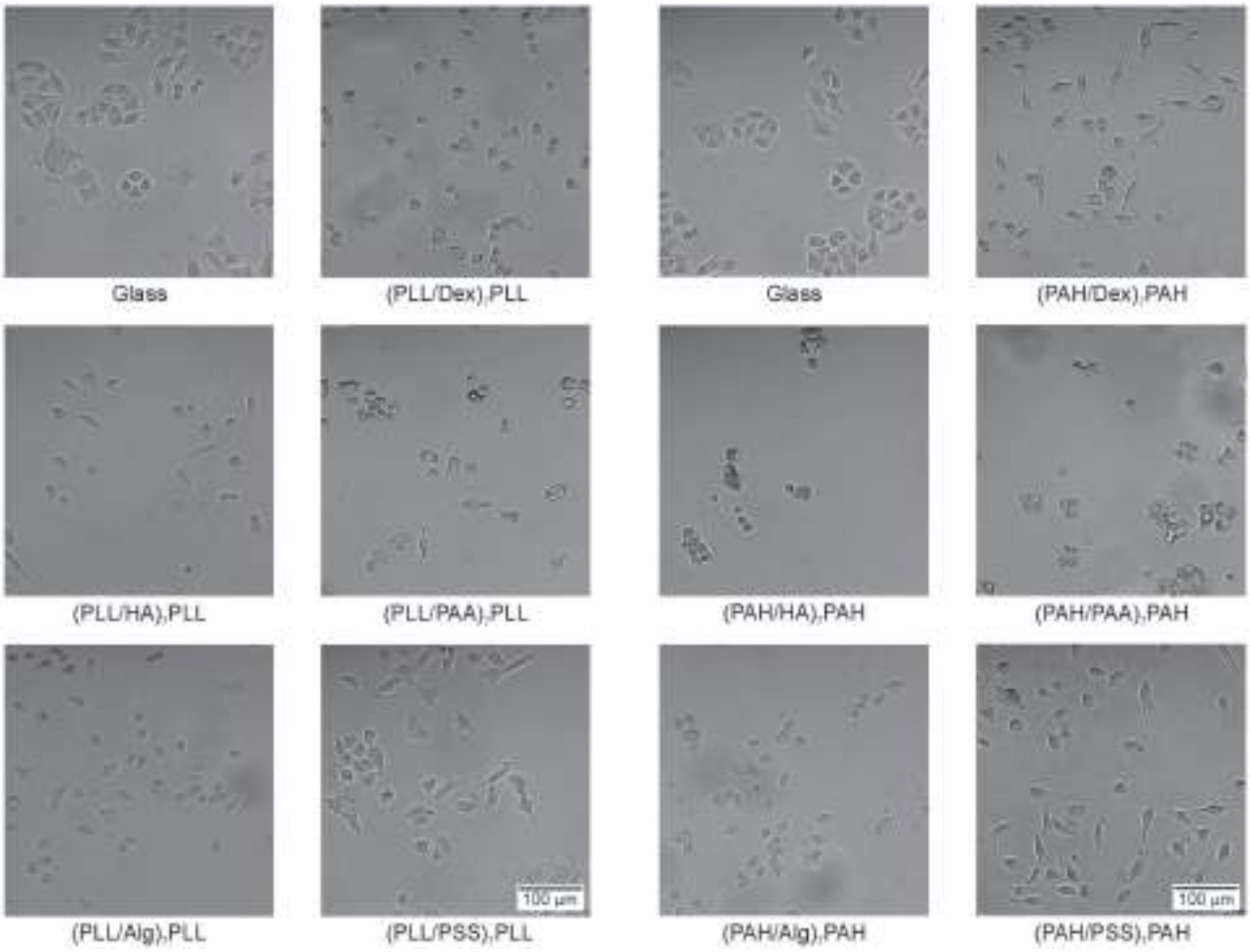

Figure 2. Microimages of A549 cells adhering on glass and PLL PEMs 48 h after seeding. The different polyanions are indicated in the corresponding microimages. The top layer is always PLL.

Figure 3. Microimages of A549 cells adhering on glass and PAH PEMs 48 h after seeding. The different polyanions are indicated in the corresponding microimages. The top layer is always PAH.

0.35–0.75 range. Similarly, for PEMs assembled with PEI and HA, ALG, DEX, and PAA cells spread less than on glass, the normalized average cell area being about 0.75 for the latter three polyanions and 0.4 for HA. On the other hand, cell spreading was promoted on PEMs assembled with PSS and all the polycations except PDADMAC. The average cell area for $(PLL/PSS)_7PLL$ and $(CHI/PSS)_7CHI$ multilayers was similar to that observed on glass, but for $(PAH/PSS)_7PAH$ the cell area had slightly smaller values. Furthermore, for $(PEI/PSS)_7PEI$ multilayers a normalized cell area of ≈1.2 was measured. Finally, PEMs assembled with PDADMAC as polycation exhibited poor cell adhesion irrespective of the polyanion, with an average normalized area close to 0.4.

The aspect ratio of cells seeded on each of the PEMs studied is shown in Figure 5. Values close to 1 indicate that cells are round and without long filopodia and adhere poorly on the substrates. On the other hand, a high value of the aspect ratio is associated with tapered cells. This interpretation is valid for cells without very rough contours or long filopodia. The average aspect ratio of cells depended on PEM composition and was compared with values obtained on glass utilizing the ANOVA test with $p = 0.05$. For PLL/ALG, PLL/DEX, PAH/PAA, and PEMs assembled with PDADMAC as polycation and all the polyanions evaluated in this work except for PSS, cells have a low average aspect ratio in comparison to glass; for the latter a value of 1.6 was observed. The smallest values for this parameter were found when cells were seeded on PEMs with PDADMAC, with the aspect ratio in the range 1.2–1.4. For PLL/HA, all PEMs assembled with CHI, PEI/HA, and PEMs assembled with PSS and all tested polycations except PAH, the values of the average aspect ratio were similar to those obtained from cells on glass. It is worth noting that the similarity in the aspect ratio of cells on PEMs and on glass correlates with good cell adhesion properties, i.e., large adhesion area, only for CHI/HA and PEMs assembled with PSS as the polyanion. For PAH based PEMs, the relative average cell area varies with the same

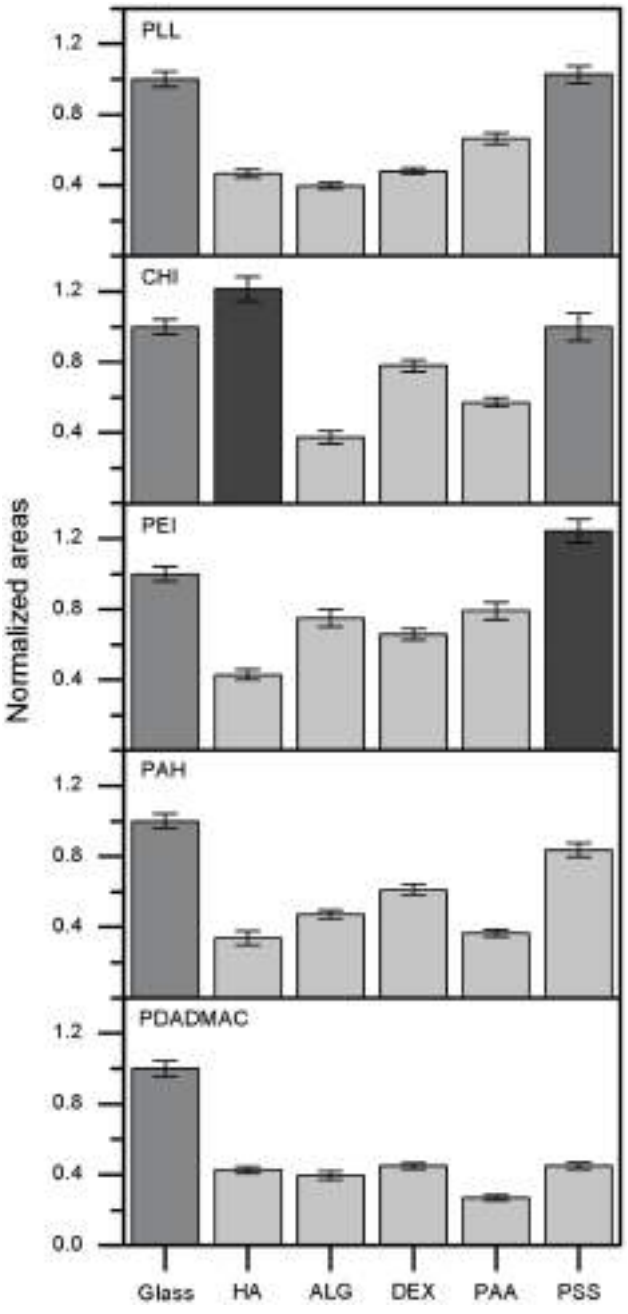

Figure 4. Normalized average cell adhesion area for A549 cells on PEMs of different composition. Each graph corresponds to a specific polycation with different polyanions; the polycation is always the top layer. Polyanions are listed in the abscise axis. At least 100 cells from four different positions of the substrate were considered for the evaluation of cell spreading area for each film. For each PEM the average cell adhesion areas were assigned to be smaller (light gray), equal (gray), or larger (dark gray) than on glass employing the ANOVA Fisher test with 0.05 significance.

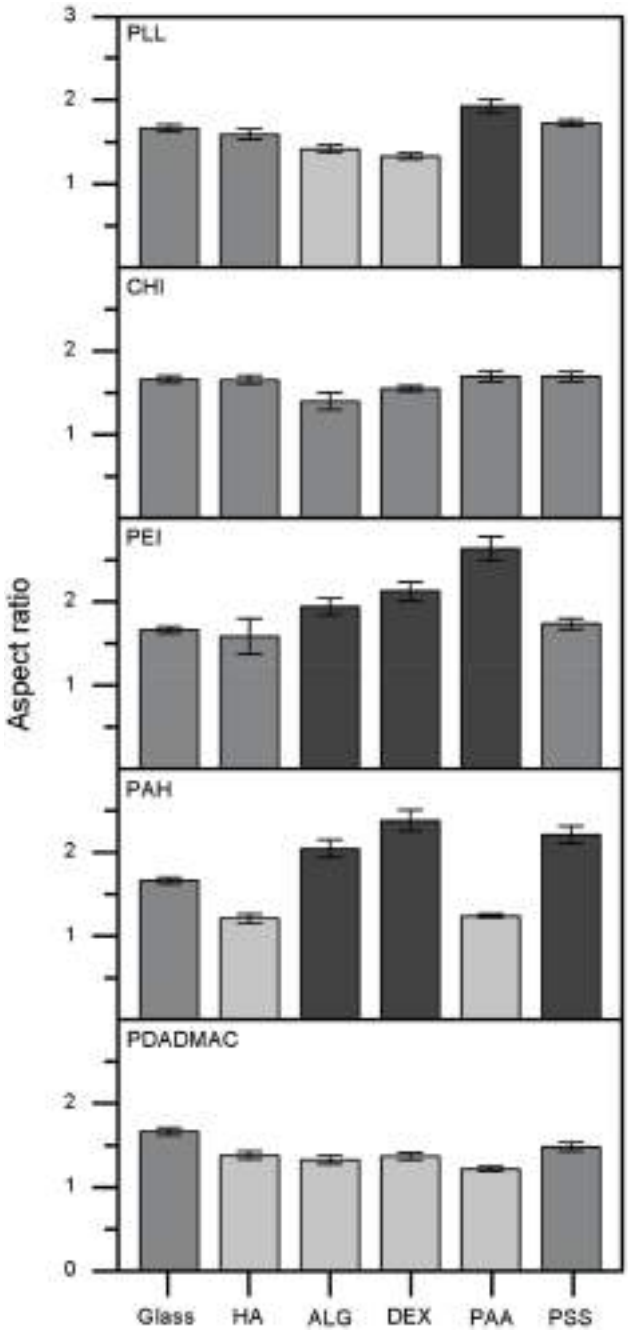

Figure 5. Morphological characteristics of A549 cells adhered on PEMs of different compositions. The top layer was always a polycation. Cell average aspect ratio is plotted for each evaluated PEM. The average aspect ratio were smaller (light gray), equal (gray), or larger (dark gray) than on glass according to the ANOVA Fisher test ($p = 0.05$).

trend as the average cell aspect ratio, the latter with a value close to that obtained on glass only for (PAH/PSS), and either smaller or higher than that obtained on glass for the other polyanions. For PEI/ALG, PEI/DEX, PEI/PAA, PAH/ALG, PAH/DEX, and PAH/PSS multilayers, values of the average cell aspect ratio in the range 1.7–2.5 were determined. The highest aspect ratio was obtained from A549 cells, which present many thin and long pseudopodia, and may suggest stressed cells due to poor interactions with the substrate.

3.1.2. Cell Proliferation

Cell viability was measured with the MTT assay 24, 48, and 72 h after seeding on the different PEMs tested in this work (Figure 6). Data showed that the viability of cells seeded on all the PEMs was smaller than for cells adhered on glass, irrespective of time, and depended on the particular PEM composition. Furthermore, viability data for different time disclosed three distinct behaviors for cell proliferation: (i) cell number increased with an exponential like behavior. This was the case of cells seeded on glass, PLL/PAA, CHI/HA, CHI/PAA, and PEMs assembled with ALG and DEX as polyanions and all tested polycations except PDADMAC/ALG, CHI/ALG, and CHI/DEX multilayers. (ii) Cell number increased linearly with time. This was observed for cells seeded on PEMs with PSS as polyanion irrespective of the polycation, CHI/ALG, CHI/DEX, and PDADMAC/ALG multilayers. (iii) The rate of cell proliferation diminished with time, a behavior observed for cells on PLL/HA, PEI/HA, PAH/HA, and PEMs assembled with PDADMAC as polycation and all the polyanions tested, except for DEX.

3.2. Diblock PEMs

With the exception of CHI/HA all other combination of biological polyelectrolytes resulted in poorer cell adhesion than the observed for PEMs of synthetic polyelectrolytes, especially than the PEMs with PSS. With the aim of increasing adhesion properties of natural biocompatible films, PEMs where assembled in the form of two blocks with two different polyelectrolyte combinations (Figure 7). The first block was formed with PSS and PLL to reinforce substrate mechanical properties and to increase cell adhesion on the resulting diblock PEMs. The topmost block was always constituted of a biopolymer combination displaying moderate cell adhesion but is biocompatible, i.e., PLL/ALG with an exponential like proliferation curve. In Figure 7 we have sketched the diblock PEMs constituted of an initial block of PLL assembled with PSS followed by an outer block of PLL assembled with ALG. The same strategy was employed to construct a diblock PEM with the same initial (PLL/PSS) block and (PLL/DEX) as the outer block (cf. the Supporting Information).

The assembly of the two blocks was studied by QCM-D as shown in Figure 8 for the first block of PLL/PSS followed by the assembly of PLL/ALG in the top layer. QCM-D data (Figure 8) show a continuous growth of the PEM for the two blocks. Data also indicate a rather supralineal growth for the (PLL/PSS) multilayer, which was grown up to 12 layers, then the growth of the subsequent $(PLL/ALG)_n PLL$ multilayer follows a lineal trend for the nine polyelectrolyte layers assembled. The PLL/ALG PEM assembled without the initial block (shown in the Supporting Information) displays supralineal growth. Accordingly, the PLL/PSS PEM seems to affect the growth of the subsequent PLL/ALG block. This fact can also be inferred from AFM imaging as well. In Figure 8c we can appreciate that the PLL/PSS PEM is quite flat and this flatness is retained by the assembly of PLL/ALG (Figure 8d). The topology of the PLL/ALG caped PEM is quite different from the pure PLL/ALG PEM shown in Figure 1, highlighting the influence of the PLL/PSS on the properties of the PLL/ALG assembled on top. QCM-D data

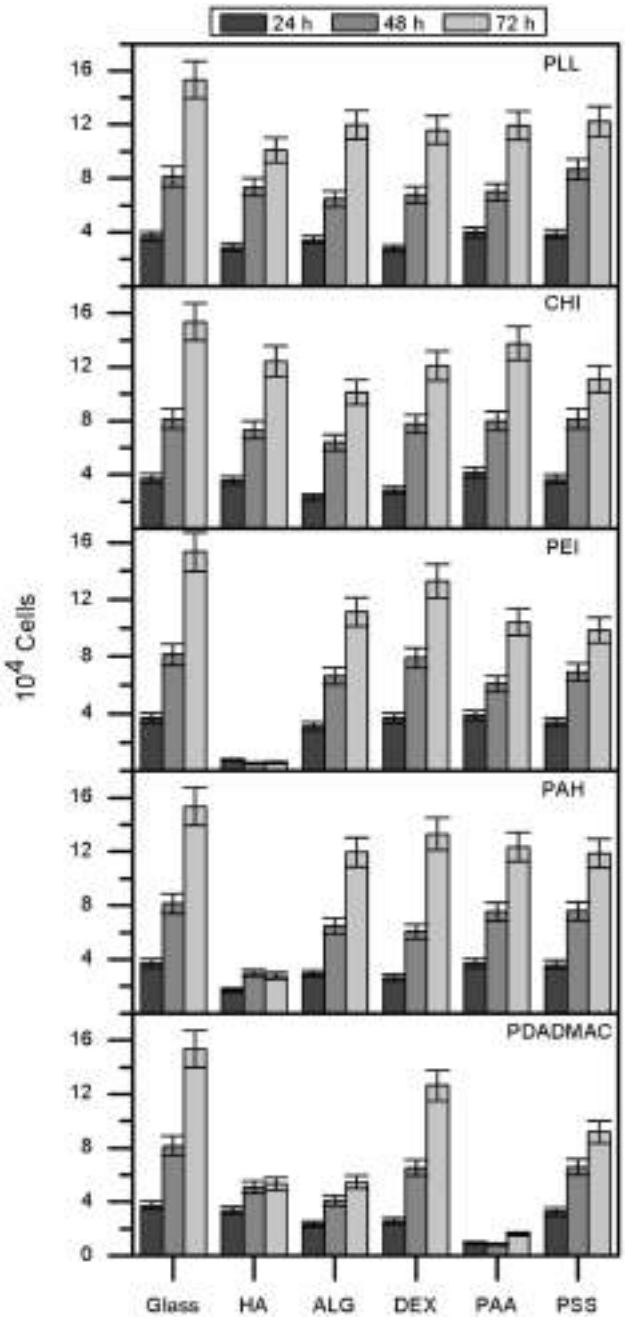

Figure 6. Cell proliferation of A549 cells on PEMs coated glass substrates measured by MTT. Cell number was measured after culturing on PEMs for 24, 48, and 72 h, as indicated in the figure. The standard deviation of the average number of cells is included.

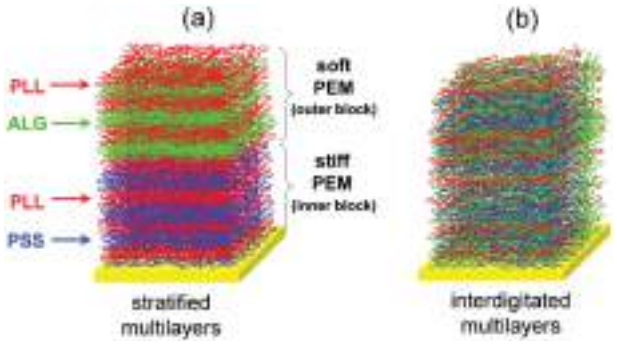

Figure 7. Scheme of a diblock polyelectrolyte multilayer. An initial PEM block of $(PLL/PSS)_6$ was first deposited, on top of which a block of a) $(PLL/ALG)_nPLL$ was assembled. Scheme (b) shows the possible interdigitation between the blocks.

and AFM images of the PLL/PSS with PLL/DEX on top are shown in the Supporting Information. PEM growth in this case is similar to the observed for the PLL/PSS and PLL/ALG as shown by the QCM-D but the assembly of PLL/DEX on top of PLL/PSS results in a rougher surface.

3.2.1. Cell Adhesion on Diblock PEMs Constituted of $(PLL/PSS)_6(PLL/ALG)_nPLL$

A549 cell adhesion on $(PLL/ALG)_nPLL$ PEMs was considerably improved when the polyelectrolytes were assembled on a (PLL/PSS)-coated substrate, forming a diblock structure, namely $(PLL/PSS)_6(PLL/ALG)_nPLL$ (Figure 9). Fluorescence images of the cell cytoskeleton and focal contacts were obtained by staining F-actin and vinculin (Figure 10). Extended cells with focal contacts formation (green spots) were observed on glass, $(PLL/PSS)_7PLL$ and $(PLL/PSS)_6(PLL/ALG)_nPLL$ (with $n = 2$ and 4). In contrast, cell seeded on $(PLL/ALG)_7PLL$ exhibited a poor cytoskeleton spreading, a few focal contacts, and a diffuse fluorescence image. From Figure 10 it can be observed that cells adhered on $(PLL/PSS)_6(PLL/ALG)_2PLL$ show longer actin fibers distributed along the cytoskeleton and larger spreading areas than cells adhered on $(PLL/PSS)_6(PLL/ALG)_4PLL$.

While the average A549 cell area on $(PLL/ALG)_7PLL$ was smaller than a half of that obtained from cells on glass, cells seeded on a diblock PEM with $n = 1$ achieved an

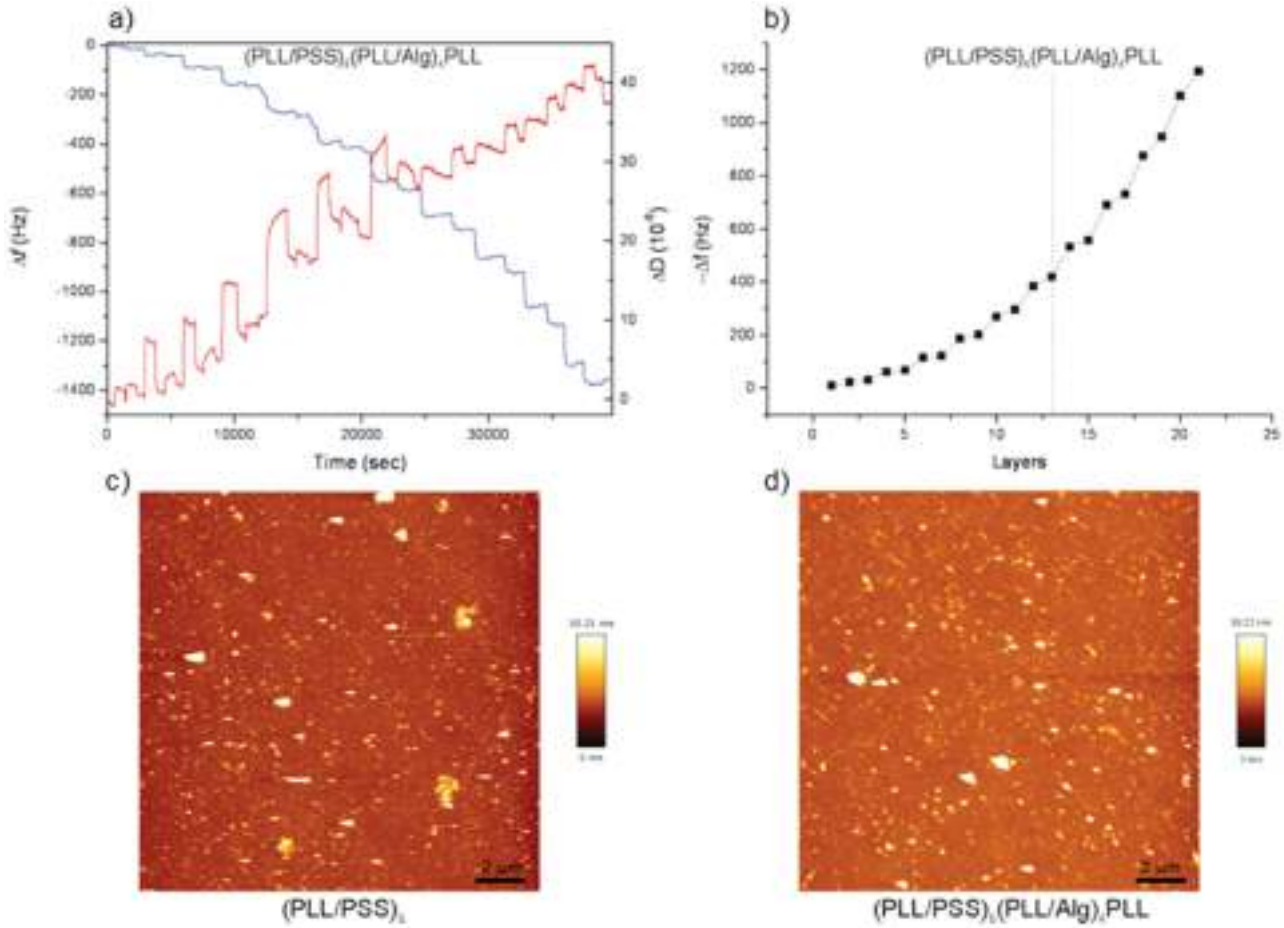

Figure 8. a) Frequency and dissipation changes as a function of the time for the assembly of $(PLL/PSS)_6(PLL/ALG)_4PLL$ multilayers. b) Corresponding absolute Frequency values as a function of the number of assembled layers. c) AFM image in dry state of $(PLL/PSS)_6$. d) AFM image in dry state of $(PLL/PSS)_6(PLL/ALG)_4PLL$.

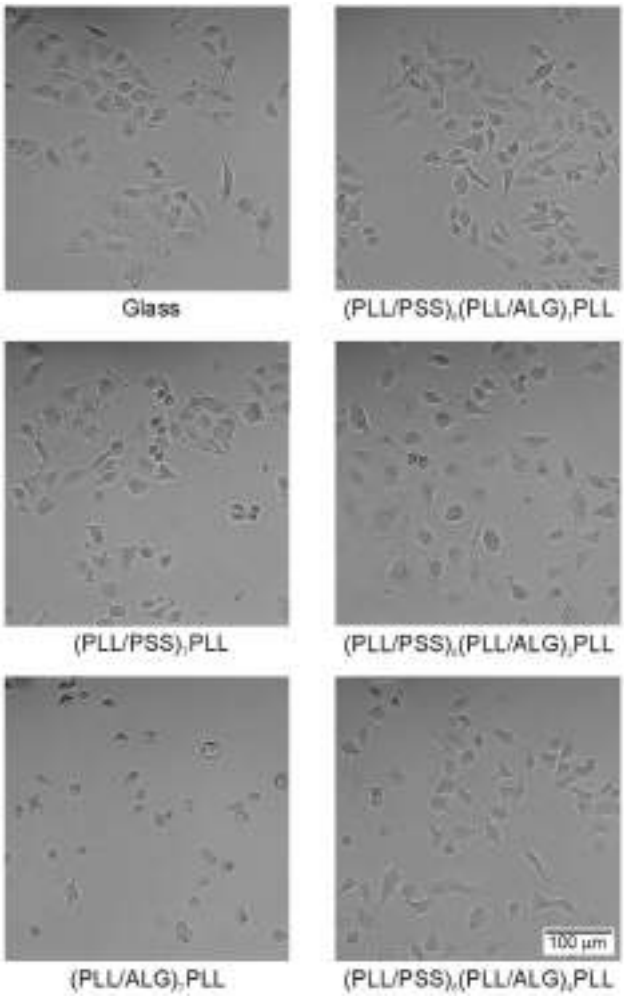

Figure 9. Microimages of A549 cells adhered on glass, $(PLL/PSS)_7PLL$ $(PLL/ALG)_7PLL$, single-block PEMs, and diblock $(PLL/PSS)_6(PLL/ALG)_nPLL$ (n = 1, 2, and 4). Microimages were taken 48 h after seeding.

average spreading area that approached that obtained on $(PLL/PSS)_7PLL$ (Figure 11). Surprisingly, cells on diblock PEMs with $n = 2$ yielded an average spreading area larger than on glass. Furthermore, with $n = 4$ the average cell spreading area decayed to a value similar to that obtained for $(PLL/PSS)_7PLL$ (Figures 9–11). Thus, the deposition of a few $(PLL/ALG)_n$ bilayers ($n = 2$) produced either an abrupt decrease or an enhancement in cell adhesion when they were directly deposited on a glass substrate (Figure 12) or a (PLL/PSS) PEM (Figure 11), respectively. For the PLL/ALG on glass the normalized cell spreading area decreased to a constant value close to 0.4 after the assemble of 3–4 (PLL/ALG) bilayers (Figure 12).

We found a similar behavior for C2C12 (mouse myoblasts) cell line than that reported above for A549 cells. An enhance in cell adhesion was observed when cells where seeded on a $(PLL/PSS)_6(PLL/ALG)_1PLL$ in comparison to each one of the blocks (cf. the Supporting Information).

4. Discussion

4.1. $(Polycation/Polyanion)_7$Polycation PEMs (Single-Block PEMs)

The data presented showed that the adhesion and proliferation of A549 cells could be modulated by PEM composition (Figures 2 and 3). Cell morphology and spreading area were related to its adhesion on PEMs. The average cell spreading area on glass, 620 ± 20 µm^2, was used as reference for presenting results of adhesion areas on the PEMs. Thus, large relative spreading areas and values of aspect ratio close to 1.5 indicated good adhesion properties. We showed that these parameters depended on the chemistry of the PEMs defined by the combination of distinct polycations and polyanions, in all the cases the polycation was the outermost layer (Figures 4 and 5). For instance PLL terminated PEMs resulted in poor adhesive surfaces when the underneath layers were assembled with the natural polyanions HA, ALG, DEX; the average cell spreading areas were below a half the value obtained on glass. These PEMs were demonstrated to grow exponentially (cf. Supporting Information Figure S1) and render relative soft composites;[36–38] PLL/HA multilayers are, for example, essentially a viscous liquid[39] with a Young modulus (E) in the range 3–85 kPa[40–42] depending on the assembling conditions. Results from our work showed that in general, except for the particular case of (CHI/HA), natural polyelectrolytes that result in softer PEMs as known from literature[43] exhibited inhibition of cell adhesion. For $(CHI/HA)_{24}$ PEMs assembled at pH = 4.5 and 0.15 M NaCl, the Young modulus resulted in E = 15 kPa.[44] Nevertheless, cells seeded on (CHI/HA) PEMs appeared to be good for cell adhesion with a spreading area 1.2 larger than for glass. The combination of biological polyanion with synthetic PEI or PAH resulted in a quite improvement in the A549 cell spreading only for certain combinations, namely, PEI/ALG, PEI/DEX, and PAH/DEX with relative average cell spreading areas in the range 0.6–0.8. In the case of PAA, its relatively high hydrophilicity[45] would explain the fact that for PEMs with PAA as polyanion, cell adhesion areas were larger than those observed on ALG or HA, but remained significantly smaller than on glass.

On the opposite situation we found that PEMs assembled with the synthetic polyanion PSS resulted in more adherent surfaces, within the timeframe of our studies; the largest relative area was obtained from cell seeded on PEI/PSS multilayers, i.e., the average cell spreading area was 1.2 times larger than on glass. Typical values of E for synthetic PEMs such as (PAH/PSS) PEMS are in the order of GPa,[46] and as expected they exhibited a linear growth (cf. Supporting Information Figure S2).

It is worth to note that the described behavior is cell type dependent, thus valid for the cell line used in this

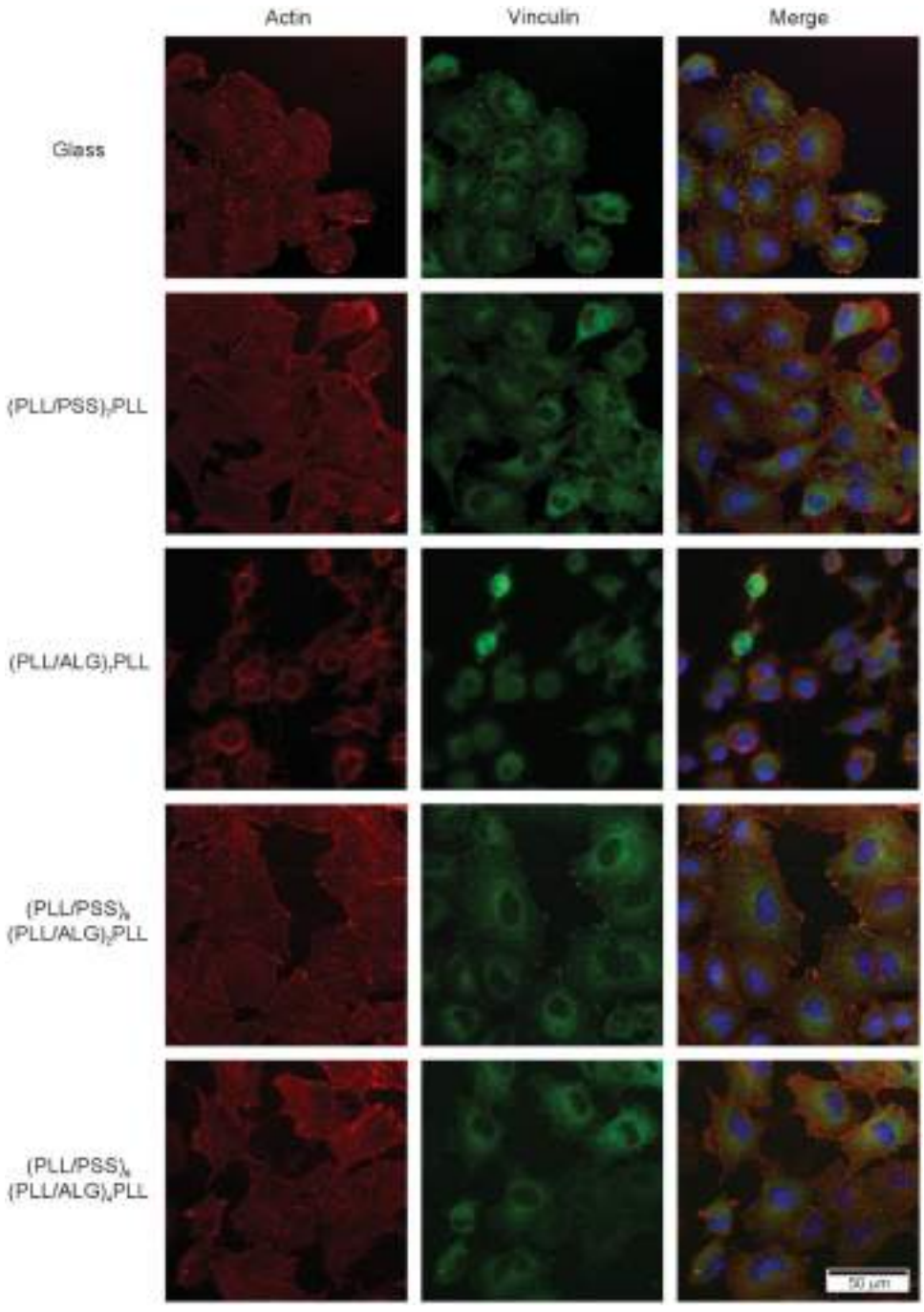

Figure 10. Fluorescence microimages of A549 cell stained for actin (red) and vinculin (green). The nuclei were also labeled with DAPI (blue). Labeling was performed 72 h after cell seeding on the substrates as indicated in the figure.

work. For instance, while adhesion of some cell lines has been demonstrated to be sensitive to the substrate stiffness, other cells appear to be nonsensitive.[47]

It is also important to keep in mind that adhesion experiments presented in this work were performed in FBS supplemented media and therefore serum proteins adsorbed on the PEM surface and partially blocked polyelectrolyte moieties that are likely to interact with cells. However, we observed differences in cell behavior seeded on each polycation terminating PEM. A cushion of proteins with different characteristics may be deposited according to the PEM composition. In this respect, it has been reported that PDADMAC-capped (PDADMAC/PSS) PEMs showed poor biocompatibility toward muscle cells even in the presence of FBS that blocked some unassociated positive PDADMAC segments.[48] Our results

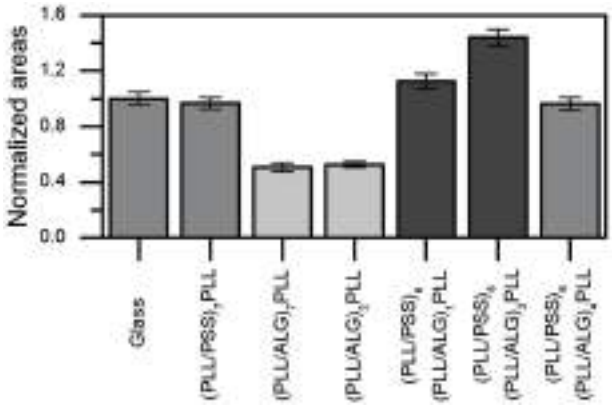

Figure 11. Normalized average cell adhesion area from A549 cells cultured for 48 h for $(PLL/PSS)_7PLL$, $(PLL/ALG)_2PLL$, $(PLL/ALG)_7PLL$ single-block PEMs, and diblock $(PLL/PSS)_6(PLL/ALG)_nPLL$ assemblies ($n = 1$, 2, and 4). At least 100 cells from four different parts of the substrate were considered for the evaluation of cell spreading area for each PEM. ANOVA test was employed to decide if average cell areas obtained on PEMs were smaller (light gray), equal (gray), or larger (dark gray) than those obtained on glass.

indicated poor A549 cell adhesion and proliferation on PEMs assembled with PDADMAC, as it was expected from the combination of the unbound segments of PDADMAC with the negative membrane proteins and phospholipids causing cytotoxicity.[48,50] Despite the above characteristics of PDADMAC, it can be used to study the effect of swelling gradients on cell migration.[51]

Cell proliferation on PEMs was assessed by MTT assay performed 24, 48, and 72 h after seeding (Figure 6). The number of cells that is proportional to the increase in the absorbance of metabolized MTT, evaluated at different time post seeding, allowed us to infer about the possible polyelectrolyte film cytotoxicity. For the experimental setup utilized in our proliferation assays, proliferation of cell was influenced by their adhesion; a lack of anchorage signaling results in a block at an early checkpoint of the

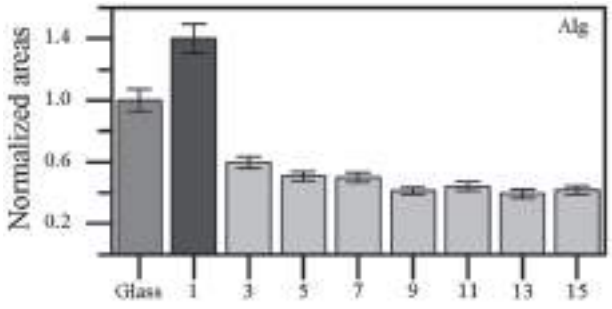

Figure 12. Normalized average cell adhesion area for $(PLL/ALG)_nPLL$ multilayers 48 h after seeding. The number of deposited layers is indicated in the abscise axis. At least 50 cells from four different parts of the substrate were considered for the evaluation of cell spreading area. Light gray, gray, and dark gray bars indicate average cell adhesion areas smaller, equal, or larger than on glass, respectively (one-way ANOVA with fisher test, $p = 0.05$).

cell cycle.[52] It has been reported for various cell types and diverse substrates that proliferation is optimal at intermediate adhesion strength, remaining quiescent when the adhesion capacity is very high.[53] Cell number for PEMs assembled with both natural polycations and polyanions, except PLL/HA, exhibited and exponential like growth, although cell spreading areas, in some cases, were smaller than on other PEMs assembled with synthetic polyanions. The proliferation rate was constant when cells were seeded on PEMs assembled with PSS and all tested polycations where good adhesion properties were found. When PDADMAC was used as polycation a sublinear relationship of the number of cells with time was obtained. PDADMAC positive chains, after serum protein absorption, appeared to inhibit cell proliferation, particularly for PEMs assembled with ALG, HA, PAA, and PSS as polyanion.[38] In summary, a change in PEM composition affected cell adhesion and proliferation differently.

Data discussed above indicate the dependence of cell functions, adhesion, and proliferation on the film composition. The latter determines the type of growth and the physical properties of the substrate, such as stiffness and wettability that cells can sense. The more biocompatible PEMs, obtained from the combination of any of the polycation PLL or CHI with any of the polyanion HA, ALG, or DEX, resulted in surfaces where cells spread more poorly than on glass, except for the $(CHI/HA)_7CHI$ multilayer. The PEMs obtained assembling either PLL or CHI with PSS resulted in more adherent surfaces for A549 cells, approaching the behavior of glass. Nevertheless, the cell number increased with a constant rate rather than with an exponential-like law. Moreover, the largest value of the relative average cell spreading area was obtained for (PEI/PSS) multilayers, although cell proliferation was hampered, and the cell number only increased linearly with time. These results would indicate that PEM composition is relevant for tuning specific cell functions properly, and could be used for designing material with particular applications.

4.2. Diblock PEMs

An appropriate PEM composition is needed to generate biocompatible materials with well-controlled adhesion properties, likely to be useful for the design of drug carrier with specific target, for tissue engineering, or to assist in wound healing processes to mention potential applications. Based on results on single PEMs (Section 4.1), PSS based PEMs display very good adhesion properties. In order to enhance cell adhesion of the biocompatible (PLL/ALG)-based PEM we decided to change the internal composition of the PEM including PSS in the first layers of the PEM without altering the top layers and surface chemistry of the PEMs which remains PLL/ALG.

Therefore, we prepared PEMs with an initial block of PEM assembled with PSS as polyanion and PLL as polycation. On top of this block a variable number of PLL/ALG or PLL/DEX bilayers (for the latter cf. the Supporting Information) were assembled as outer block. In this way we assure that the surface of the film remains biocompatible. The combination of $(PLL/PSS)_6$ with $(PLL/ALG)_n$ or $(PLL/DEX)_n$ forming a diblock system resulted in an enhancement in cell adhesion properties compared to $(PLL/ALG)_n$ or $(PLL/DEX)_n$-coated glass for the same number of multilayers (Figures 9–12). Furthermore for DEX and ALG based PEMs, larger adhesion areas were obtained for $n = 2$ than for 1 or 4 (Figure 11). The relative adhesion area resulted in 1.2 for $(PLL/PSS)_6(PLL/ALG)_2PLL$, a figure larger than that obtained from each one of the single blocks utilized to generate the diblock system (Figures 11 and 12). Furthermore, immunostaining microimages of cells (Figure 10) seeded on $(PLL/ALG)_7PLL$ exhibited a diffuse actin cytoskeleton and no evidence of vinculin adhesion protein recruitment forming focal adhesion contacts. On the other hand, cell seeded on glass or diblock PEMs showed stress fibers and the formation of focal adhesion that maintain the cell cytoplasm extended and under tension, a fact that is more remarkable for $(PLL/PSS)_6(PLL/ALG)_2PLL$, in agreement with the trends indicated by the normalized cell adhesion areas.

Diblock PEMs appeared to have different properties toward cell adhesion and proliferation than those observed on each single-block PEMs. This fact is in agreement with the idea that polyelectrolyte interdigitation during assembling or in the post assembling stage is conferring physicochemical properties, which are not found on each block system individually. In other words PSS molecules from the inner block are likely to be present in the outer block as well as ALG molecules are present in the inner block (Figure 7). QCM-D and AFM data indicated that the growth and morphology of (PLL/ALG) or (PLL/DEX) PEMs were different depending on whether they were deposited on glass or on an underneath (PLL/PSS) film (Figure 8 and Figure S3, Supporting Information).

Interdigitation is a well-known phenomenon in PEMs and has been described in previous articles.[54–57] When a polyelectrolyte layer is assembled in a PEM it can affect the film up to four layers below. This process takes place in PEMs with thickness increasing either linearly or supralinearly.[58] Even in linear relatively compact growing PEMs the newly adsorbed layers interdigitate into some top layers.[59] It has been reported that roughness is smaller next to the film/air interface and increases with the number of bilayers inward,[58] a fact that has been explained by the supporting layer interdiffusion promoted by each new deposition step.

The consequence of the interdigitation is that the properties of the outer block are different from those of the same block assembled on glass. When the number of PEMs in the outer block increases over four to six bilayers, the effects of the inner block decrease and cell adhesion starts to decrease. Addition of more layers of polyelectrolytes on the outer block promotes further decrease of adhesion, thus suggesting that after four to six bilayers deposition, interdigitation is no longer playing a significant role.

Interdigitation experiments provide a simple means to tune adhesion in multilayers by preparing them as blocks keeping the surface chemistry of the film almost unaltered. In this way, our results showed that biocompatible surfaces with improved adhesion can be achieved as, for example, in films with the glassy PSS, due to its high Elastic module. On the other hand the experiments proved how important the mechanical properties of the film are in determining adhesion. For the same surface chemistry if the mechanical properties of the film are changed adhesion can also change.

5. Conclusions

The effect of PEM chemistry on A549 cell adhesion and proliferation was studied by comparing cell behavior, cellular area, and morphology on glass and on PEMs with different compositions.

Polyelectrolytes of natural and synthetic origin were employed to assemble polycation-terminated PEMs with a constant number of polyelectrolyte layers. In general, soft PEMs with a supralinear growth resulted in substrates with poor cell adhesion properties. Furthermore, PEMs assembled with the glassy PSS polyanion and each polycation except PDADMAC resulted in much more adherent surfaces. For instance, for PEI/PSS PEMs a normalized spreading area of 1.2 was determined.

On the other hand, we observed that the change in PEM composition affects cell adhesion characteristics and proliferation differently. Particularly, for PEMs with PSS and good cell adhesion properties, cell number increases with time following a linear relationship instead of an exponential-like law.

For each PEM with a defined terminal polycation, even in the presence of adhered proteins from the culture medium, cells are able to sense physical and chemical properties impaired by varying the polyanion at inner layers. The different polyelectrolyte combination employed in the assembling process generates PEMs with a constant number of layers but with varying physical and chemical properties that can be sensed by the cells. Thus, differences in film thickness, stiffness, the cushion of adsorbed proteins from the culture medium, and the intrinsic moieties of each polyelectrolyte are reflected in differences in cell behavior toward adhesion and proliferation.

In the case of diblock PEMs, interdigitation between the polyelectrolytes of the inner and outer blocks would generate an interface with properties different than those of each one of the blocks deposited on glass. These changes in film properties can be sensed by cells up to four to six bilayers of the outer block. The fabrication of diblock PEMs offers a simple and easy procedure for engineering surfaces to modulate cell adhesion by the precise combination of single blocks of PEMs to generate biocompatible complex substrates.

Supporting Information

Supporting Information is available from the Wiley Online Library or from the author.

Acknowledgements: This work was supported by the European Commission in the framework of FP7 PEOPLE-2009 Project TRASNADE Proposal No: 247656. The authors also acknowledge the project MAT2013-48169-R from the Spanish Ministry of Economy (MINECO), Consejo Nacional de Investigaciones Científicas y Técnicas (CONICET, Argentina) (Grant No. PIP 0602), Agencia Nacional de Promoción Científica y Tecnológica (ANPCyT, Argentina; PICT-163/08, PICT-2010-2554, and PICT-2013-0905), the Austrian Institute of Technology GmbH (AIT–CONICET Partner Group: "Exploratory Research for Advanced Technologies in Supramolecular Materials Science," Exp. 4947/11, Res. No. 3911, 28-12-2011), and Universidad Nacional de La Plata (UNLP). M.A.P. and O.A. are staff members of CONICET.

Received: July 20, 2015; Revised: October 9, 2015; Published online: December 11, 2015; DOI: 10.1002/mabi.201500275

Keywords: adhesion; biocompatibility; mechanical properties; polyelectrolytes; tissue engineering

[1] L. Bacakova, E. Filova, M. Parizek, T. Ruml, V. Svorcik, *Biotech. Adv.* **2011**, *29*, 739.
[2] A. Engler, L. Bacakova, C. Newman, A. Hategan, M. Griffin, D. Discher, *Biophys. J.* **2004**, *86*, 617.
[3] P. M. Kharkar, K. L. Kiick, A. M. Kloxin, *Chem. Soc. Rev.* **2013**, *42*, 7335.
[4] S. Saxena, M. W. Spears Jr., H. Yoshida, J. C. Gaulding, A. J. García, L. A. Lyon, *Soft Matter* **2014**, *10*, 1356.
[5] M. B. Baker, C. S. Chen, *J. Cell Sci.* **2012**, *125*, 1.
[6] F. Boulmedais, V. Ball, P. Schwinte, B. Frisch, P. Schaaf, J. Voegel, *Langmuir* **2003**, *19*, 440.
[7] J. Borges, J. F. Mano, *Chem. Rev.* **2014**, *114*, 8883.
[8] J. Zhou, G. Romero, E. Rojas, L. Ma, S. Moya, C. Gao, *J. Colloid Interface Sci.* **2010**, *345*, 241.
[9] J. Almodóvar, R. Guillot, C. Monge, J. Vollaire, *Biomaterials* **2014**, *35*, 3975.
[10] F. Gorouhi, N. M. Shah, V. Krishna Raghunathan, Y. Mohabbati, N. L. Abbott, R. R. Isseroff, C. J. Murphy, *J. Invest. Dermatol.* **2014**, *134*, 1757.
[11] S. Schmidt, N. Madaboosi, K. Uhlig, D. Köhler, A. Skirtach, C. Duschl, H. Möhwald, D. V. Volodkin, *Langmuir* **2012**, *28*, 7249.
[12] D. Volodkin, A. Skirtach, H. Möhwald, *Adv. Polym. Sci.* **2011**, *240*, 135.
[13] J. M. Mets, J. T. Wilson, W. Cui, E. L. Chaikof, *Adv. Healthcare Mater.* **2013**, *2*, 266.
[14] R. R. Costa, J. F. Mano, *Chem. Soc. Rev.* **2014**, *43*, 3453.
[15] V. Gribova, R. Auzely-Velty, C. Picart, *Chem. Mater.* **2012**, *24*, 854.
[16] T. Crouzier, T. Boudou, C. Picart, *Curr. Opin. Colloid Interface Sci.* **2010**, *15*, 417.
[17] S. Jain, D. Kumar, N. K. Swarnakar, K. Thanki, *Biomaterials* **2012**, *33*, 6758.
[18] M. L. Manca, D. Valenti, O. D. Sales, A. Nacher, A. M. Fadda, M. Manconi, *Int. J. Pharm.* **2014**, *472*, 102.
[19] D. Volodkin, R. von Klitzing, H. Moehwald, *Polymers* **2014**, *6*, 1502.
[20] E. Lih, S. H. Oh, Y. K. Joung, J. H. Lee, D. K. Han, *Prog. Polym. Sc.* **2015**, DOI: 10.1016/j.progpolymsci.2014.10.004.
[21] N. Saha, C. Monge, V. Dulong, C. Picart, K. Glinel, *Biomacromolecules* **2013**, *14*, 520.
[22] E. di Martino, G. Kelly, J. A. Roulson, M. A. Knowles, *Mol. Cancer Res.* **2015**, *13*, 138.
[23] F. Rehfeldt, A. J. Engler, A. Eckhardt, F. Ahmed, D. E. Discher, *Adv. Drug Delivery Rev.* **2007**, *59*, 1329.
[24] J. D. Mih, A. Marinkovic, F. Liu, A. S. Sharif, D. J. Tschumperlin, *J. Cell Sci.* **2012**, *125*, 5974.
[25] J. M. Paszek, M. Zahir, R. K. Johnson, J. N. Lakins, G. I. Rozenberg, A. Gefen, C. A. Reinhart-King, S. S. Margulies, M. Dembo, D. Boettiger, D. A. Hammer, V. M. Weaver, *Cancer Cell* **2005**, *8*, 241.
[26] H. Chang, H. Zhang, M. Hu, X. Chen, K. Ren, J. Wang, J. Ji, *Biomater. Sci.* **2015**, *3*, 352.
[27] S. Mehrota, S. C. Hunley, K. M. Pawelec, L. Zhang, I. Lee, S. Baek, C. Chan, *Langmuir* **2010**, *3*, 12794.
[28] A. G. Skirtach, D. V. Voldkin, H. Möhwald, *ChemPhysChem* **2010**, *11*, 822.
[29] G. Francius, J. Hemmerlé, V. Ball, P. Lavalle, C. Picart, J. Voegel, P. Schaaf, B. Senger, *J. Phys. Chem. C.* **2007**, *111*, 8299.
[30] L. Kocgozlu, P. Lavalle, G. Koening, B. Senger, Y. Haikel, P. Schaaf, J. C. Voegel, H. Tenenbaum, D. Vautier, *J. Cell Sci.* **2010**, *123*, 29.
[31] M. Salomaki, J. Kankare, *Biomacromolecules* **2009**, *10*, 294.
[32] T. Boudou, T. Crouzier, K. Ren, G. Blin, C. Picart, *Adv. Mater.* **2009**, *22*, 441.
[33] A. L. Hillberg, C. A. Holmes, M. Tabrizian, *Biomaterials* **2009**, *30*, 4463.
[34] L. Han, Z. Mao, J. Wu, Y. Guo, T. Ren, C. Gao, *Biomaterials* **2013**, *34*, 975.
[35] K. Ren, L. Fourel, C. G. Rouvière, C. Albiges-Rizo, C. Picart, *Acta Biomater.* **2010**, *6*, 4238.
[36] C. Picart, J. Mutterer, L. Richert, Y. Luo, G. D. Prestwich, P. Schaaf, P. Lavalle, *Proc. Natl. Acad. Sci. USA* **2002**, *99*, 12531.
[37] D. L. Elbert, C. B. Herbert, J. A. Hubbell, *Langmuir* **1999**, *15*, 5355.
[38] P. Lavalle, C. Picart, J. Metterer, C. Gergely, H. Reiss, J. C. Voegel, B. Senger, P. Schaaf, *J. Phys. Chem. B* **2004**, *108*, 635.
[39] C. Picart, B. Senger, K. Sengupa, F. Dubreuil, A. Fery, *Colloids Surf. A* **2007**, *303*, 30.
[40] A. J. Englera, R. Ludovic, J. Y. Wong, C. Picart, D. E. Discher, *Surf. Sci.* **2004**, *570*, 142.
[41] A. Schneider, G. Francius, R. Obeid, P. Schwinté, J. Hemmerlé, B. Frisch, P. Schaaf, J. C. Voegel, B. Senger, C. Picart, *Langmuir* **2006**, *22*, 1193.
[42] S. Schmidt, N. Madaboosi, K. Uhlig, D. Köhler, A. Skirtach, C. Duschl, H. Möhwald, D. V. Volodkin, *Langmuir* **2012**, *28*, 7249.

[43] L. Richert, A. J. Engler, D. E. Discher, C. Picart, *Biomacromolecules* **2004**, *5*, 1908.
[44] A. Schneider, L. Richert, G. Francius, J. C. Voegel, C. Picart, *Biomed. Mater.* **2007**, *2*, 45.
[45] D. S. Salloum, S. G. Olenych, C. S. Keller, J. B. Schelenoff, *Biomacromolecules* **2005**, *6*, 161.
[46] A. J. Nolte, N. D. Treat, R. E. Cohen, M. F. Rubner, *Macromolecules* **2008**, *41*, 5793.
[47] R. W. Tilghman, C. R. Cowan, J. D. Mih, Y. Koryakina, D. Gioeli, J. K. Slack-Davis, J. T. Parsons, *PLoS One* **2010**, *5*, e12905.
[48] L. Han, Z. Mao, J. Wu, Y. Zhang, C. Gao, *Interface* **2012**, *9*, 3455.
[49] D. Fischer, Y. X. Li, B. Ahlemeyer, J. Krieglstein, T. Kissel, *Biomaterials* **2003**, *24*, 1121.
[50] H. Murata, R. R. Koepsel, K. Matyjaszewski, A. J. Russell, *Biomaterials* **2007**, *28*, 4870.
[51] L. Han, Z. Mao, J. Wu, Y. Guo, T. Ren, C. Gao, *Biomaterials* **2013**, *34*, 975.
[52] R. K. Assoian, E. A. Klein, *Trends Cell. Biol.* **2008**, *18*, 347.
[53] L. Bacakova, E. Filova, F. Rypacek, V. Svorcik, V. Stary, *Physiol. Res.* **2004**, *53*, S35.
[54] G. Decker, *Science* **1997**, *277*, 1232.
[55] M. C. Hsieh, R. J. Farris, T. J. McCarthy, *Macromolecules* **1997**, *30*, 8453.
[56] E. Donath, D. Walther, V. N. Shilov, E. Knippel, A. Budde, K. Lowack, C. A. Helm, H. Möhwald, *Langmuir* **1997**, *13*, 5294.
[57] F. Caruso, H. Lichtenfeld, E. Donath, H. Möhwald, *Macromolecules* **1999**, *32*, 2317.
[58] G. Ladam, P. Schaad, J. C. Voegel, P. Schaaf, G. Decher, F. Cuisinier, *Langmuir* **2000**, *16*, 1249.
[59] O. Soltwedel, O. Ivanova, P. Nestler, M. Müller, R. Köhler, C. A. Helm, *Macromolecules* **2010**, *43*, 7288.